Design of BLDC Motor Controller for Electric Power Wheelchair

Jun-Uk Chu, In-Hyuk Moon, Gi-Won Choi, Jei-Cheong Ryu, and Mu-Seong Mun

Korea Orthopedics and Rehabilitation Engineering Center, Incheon, Korea
(Tel : +82-32-500-0597; E-mail: juchu@iris.korec.re.kr)

Abstract: The electric power wheelchair needs to control motor torque and speed for responding to variable actions given by handling a joystick. In this paper a DSP-based BLDC motor controller using a single dc-link current sensor is presented for electric power wheelchair. It is composed by a DSP processor and three-phase inverter module. To control torque, high speed current control is achieved by the PI controller and pulse width modulation (PWM) signals with 25 kHz carrier frequency, which is performed by 200 $m$sec cycle. The speed controller computes the new direct current reference from the speed error and the PI control equation. The displacement value by handling the joystick is converted to reference speeds of right and left wheel motors using nonholonomic wheelchair kinematics. Experimental results show that the presented control system is enough to implement a speed servo in wheelchair driving.

Keywords: electric power wheelchair, BLDC motor, current and speed control, joystick

1. INTRODUCTION

Recently, the demand of electric power wheelchair has increased in silver and rehabilitation area. An electric power wheelchair is composed of several parts: user interface, integrated controller, power system, and motor. The joystick is the most common control interface between the user and the wheelchair. Integrated control is used to facilitate using the joystick to control power system and motor. To implement the power system for motor driving, a servo-amplifier is required to convert signal level given by integrated controller to motor power.

There are several motor types to be applied to electric power wheelchair. Most current designs use permanent magnet direct current (dc) motors. These motors provide high torque and easy control. However the traditional gear driven dc motor system is constrained by the limitations of the mechanical speed reducing device. A machine built in this way has to pay performance penalties in acceleration, accuracy, repeatability and efficiency.

Alternating current (ac) motors are designed to be highly efficient and controlled with modern power circuitry. Because of the development and wide dissemination of switching inverter techniques, it is quite feasible to use ac motors with a battery supply. To date, ac motors have been used in research on power wheelchairs. As one of the ac motors, BLDC motor has been used as an actuator in many applications.

In this study, a DSP-based BLDC motor controller using a single dc-link current sensor is presented for electric power wheelchair. It is composed by a DSP processor and three-phase inverter module. The BLDC motor employed in this study is a pancake type with 250W performance and it has a planetary reduction system with a low gear ratio. The key to effective torque and speed control of the BLDC motor is based on relatively simple torque and Back EMF equations, which are similar to those of the dc motor. The current sensing is ensured by a low cost shunt resistor, and used for over-current protection and current feedback. The current control is achieved by the PI controller and pulse width modulation (PWM) signals with varying duty rates. Hall effect sensors are available to detect the rotor shaft position, and used for electronic commutation and speed feedback. The speed controller computes the new direct current reference from the speed error and the PI control equation. The position of joystick is represented by a pair of radius and angle. The linear and angular velocity of wheelchair are a normalized function of angle, and scaled by radius. Using nonholonomic wheelchair kinematics, these values are converted to reference speeds of right and left wheel motors.

By experimental results, it can be verified that the system is enough as a speed servo in wheelchair driving.

2. BLDC MOTOR

Permanent magnet synchronous machines with trapezoidal-EMF and rectangular stator currents are widely used as they offer the following advantages: first, assuming the motor has pure trapezoidal Back EMF and that the stator phases commutation process is accurate, the mechanical torque developed by the motor is constant; secondly, the Brushless DC drives show a very high mechanical power density. The BLDC motor in this study is a pancake type with 250W performance, and used with a planetary gear reduction system. It has eight magnetic pole pairs on the rotor and three-phase start-connection. The equivalent circuit of BLDC motor is shown in Fig. 1.

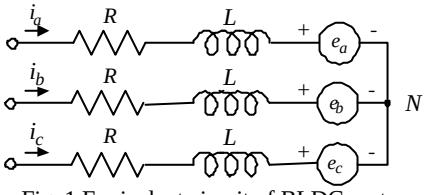

Fig. 1 Equivalent circuit of BLDC motor.

The voltage equation of BLDC motor can be represented as

$$\begin{bmatrix} V_a \\ V_b \\ V_c \end{bmatrix} = \begin{bmatrix} R & 0 & 0 \\ 0 & R & 0 \\ 0 & 0 & R \end{bmatrix} \begin{bmatrix} i_a \\ i_b \\ i_c \end{bmatrix} + \begin{bmatrix} L & 0 & 0 \\ 0 & L & 0 \\ 0 & 0 & L \end{bmatrix} \frac{d}{dt} \begin{bmatrix} i_a \\ i_b \\ i_c \end{bmatrix} + \begin{bmatrix} e_a \\ e_b \\ e_c \end{bmatrix} \quad (1)$$

where R is phase resistance, L is phase inductance, V_a, V_b, V_c are phase voltages, i_a, i_b, i_c are phase currents, and e_a, e_b, e_c are back EMFs.

The generated torque of the motor is given by

$$T = \frac{e_a i_a + e_b i_b + e_c i_c}{w} \quad (2)$$

where w is the motor's angular velocity.

3. CONTROL HARDWARE

The control hardware is composed by DSP and three-phase inverter module. The proposed controller utilizes a DSP processor, TMS320LF2407A. The processor is a single chip solution based on a 20 MIPS 16-bit fixed-point DSP core associated with several micro-controller peripherals such as a pulse width modulation (PWM) generator and analog to digital converters (ADC).

In three-phase inverter module, the power switches use the power MOSFET, type IRF1010E. The selected pre-driver component is the IR2101 and the PWM output signals coming from TMS320LF2407A are directly connected to the pre-driver. The pre-driver output signals go through a resistor and then directly to the power switches. Two independent pairs of PWM generator are used for right and left wheel motors.

The current sensing is ensured by a low cost shunt resistor, its voltage drop is directly interfaced with the ADC module and used for over-current protection and current feedback.

The motor is equipped with three Hall effect sensors. The sensor outputs are directly wired to the TMS320LF2407A Capture Unit. It is available to detect the rotor shaft position, and used for electronic commutation and speed feedback.

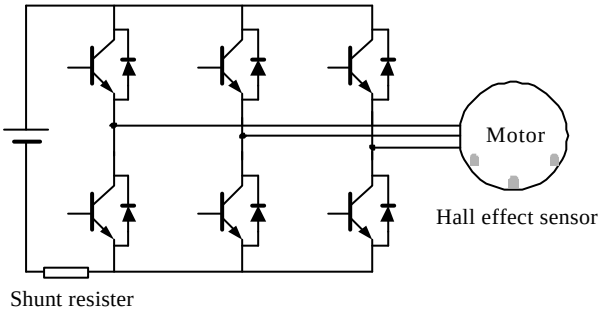

Fig. 2 Three-phase inverter module.

4. CONTROL STRUCTURE

The key to effective torque and speed control of a BLDC motor is based on relatively simple torque and Back EMF equations, which are similar to those of the DC motor. The Back EMF magnitude can be written as

$$E = 2N\ lrBw \tag{3}$$

and the torque term as

$$T = \left(\frac{1}{2} i^2 \frac{dL}{dq}\right) - \left(\frac{1}{2} B^2 \frac{dR}{dq}\right) + \left(\frac{4N}{p} Brlpi\right) \tag{4}$$

where N is the number of winding turns per phase, l is the length of the rotor, r is the internal radius of the rotor, B is the rotor magnet flux density, w is the motor's angular velocity, i is the phase current, L is the phase inductance, q is the rotor position, R is the phase resistance. The first two terms in the torque expression are parasitic reluctance torque components. The third term produces mutual torque, which is the torque production mechanism used in the case of BLDC motors. To sum up, the Back EMF is directly proportional to the motor speed and the torque production is almost directly proportional to the phase current. These factors lead to the following BLDC motor speed control scheme.

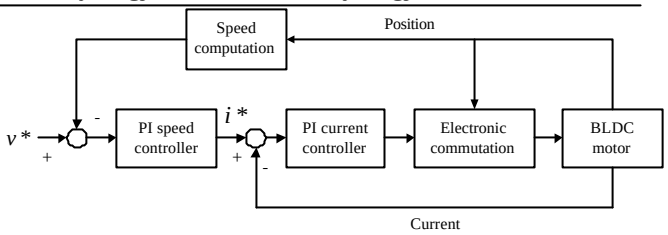

Fig. 3 Speed and current control scheme.

In this control scheme, torque production follows the principle that current should flow in only two of the three phases at a time. Only one current at a time needs to be controlled so that only one current sensor is necessary. The positioning of the current sensor allows the use of a low cost sensor as a shunt.

4.1 Electronic commutation

The Hall effect sensors give three 180°(electrical degree) overlapping signals, thus providing the six mandatory commutation points. The rising and falling edges of the sensor output are detected, the corresponding interrupt flag is generated and the Interrupt Sub Routine is served. The ISR first determines which edge has been detected, and then commutates the supplied phases.

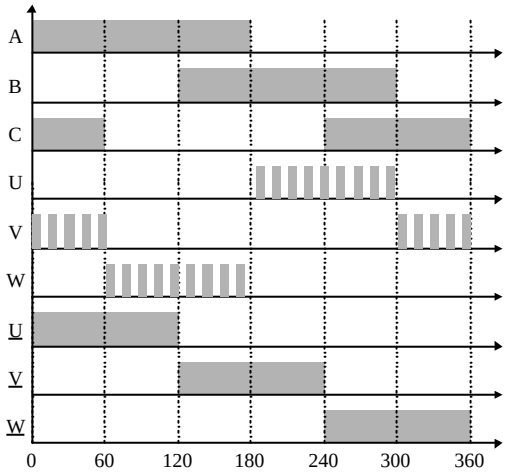

Fig. 4 Commutation sequence.

4.2 Current control

As shown in Figure 2, a shunt resistor is used to sense the current. The shunt is inserted between the sources of the power bridge lower side and the power board ground. Its value is set such that it activates the integrated over-current protection when the maximum current permitted by the power board has been reached. The voltage drop across the shunt resistor is converted by the dual ADC module, once it has been amplified to address the whole conversion range. The end of the conversion generates an interrupt flag and the Interrupt Sub Routine is executed. The ADC reading for 45A will be 3FFh and for 0A will be 0h. The phase current is sensed every 40 $m$sec in order to implement a 200 $m$sec current loop. Each current controller leads to a new duty cycle loaded at the beginning of a PWM cycle. Current control is achieved by Pulse Width Modulation (fixed frequency 25kHz) signals with varying duty cycles. PWM width is determined by comparing the measured phase current

with the desired reference current. The PI current controller is

$$e_i(k) = i^*(k) - i(k)$$
$$d(k) = d(k-1) + K_i^p\left(e_i(k) - e_i(k-1)\right) + K_i^i e_i(k) \quad (5)$$

where i^* is the reference current, i is the actual current, e_i is the current error, d is the PWM duty, K_i^p is the proportional gain, and K_i^i is the integral gain.

4.3 Speed control

The speed feedback is derived from the position sensor output signals. As mentioned, there are six commutation signals per electrical revolution. In our motor, between two commutation signals there are 22.5° mechanical degrees. As the speed can be written as

$$\frac{\Delta X}{\Delta t} \quad (6)$$

where ΔX is the arc of the radius of wheel related to 22.5° mechanical degrees. It is possible to get the speed from the computed elapsed time Δt between two captures. Between two commutation signals the angle variation is constant as the Hall effect sensors are fixed relative to the motor, so speed sensing is reduced to a simple division.

The speed control loop is executed once every 10 msec. The new direct current reference is computed from the speed error and the PI control equation given by

$$e_v(k) = v^*(k) - v(k)$$
$$i^*(k) = i^*(k-1) + K_v^p\left(e_v(k) - e_v(k-1)\right) + K_v^i e_v(k) \quad (7)$$

where v^* is the reference speed, v is the actual speed, e_v is the speed error, K_v^p is the proportional gain, and K_v^i is the integral gain.

4.4 Reference speed computation

The position of joystick is represented by a pair of radius r and angle q as shown in Fig. 5 The linear and angular velocities of wheelchair are a normalized function of angle, and scaled by radius. This equation is represented by

$$v_t = \frac{r}{2}\cos\left(\frac{2p}{p-2a}\left(q - \frac{p}{2}\right)\right) + \frac{r}{2}, \quad a < q < p - a \quad (8)$$
$$v_t = 0, \quad p - a < q < -p + a$$
$$v_t = -\frac{r}{2}K_b\cos\left(\frac{2p}{p-2a}\left(q + \frac{p}{2}\right)\right) + \frac{r}{2}, \quad -p + a < q < -a$$
$$v_t = 0, \quad -a < q < a$$
$$w_t = -\frac{r}{2}\cos 2q + \frac{r}{2}, \quad -\frac{p}{2} < q < \frac{p}{2}$$
$$w_t = \frac{r}{2}\cos 2q + \frac{r}{2}, \quad \frac{p}{2} < q, \quad q < -\frac{p}{2}$$

where K_b is the backward gain. The normalized linear and angular velocities are shown in Fig. 6(a).

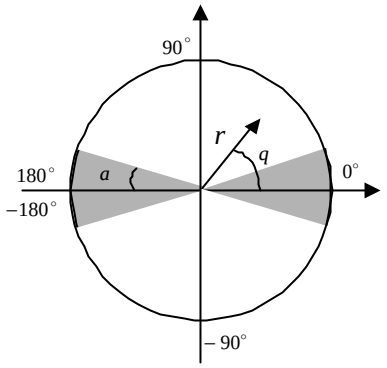

Fig. 5 Joystick position.

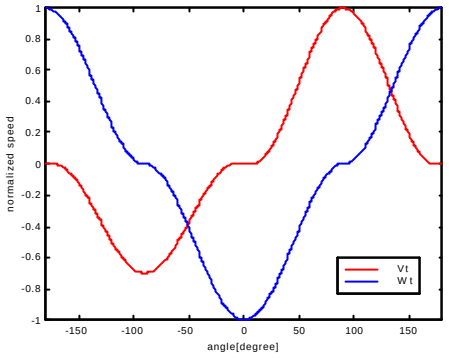

(a)

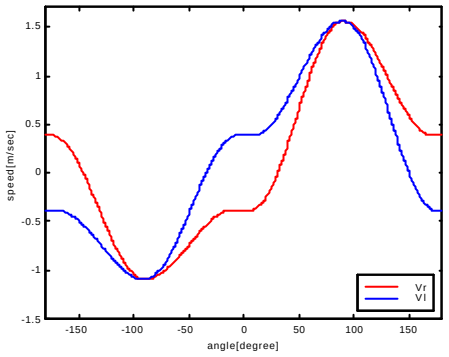

(b)

Fig. 6 (a) Normalized linear and angular velocity, (b) Reference speeds of right and left wheel motors.

Using nonholonomic wheelchair kinematics these values are converted to reference speeds of right and left wheel motors as shown in Fig. 6 (b).

$$v_r^* = K_l v_t + \frac{W}{2}K_a w_t$$
$$v_l^* = K_l v_t - \frac{W}{2}K_a w_t \quad (9)$$

where v_t is the linear velocity of wheelchair, w_t is the angular velocity of wheelchair, v_r is the reference speed of right wheel motor, and v_l is the reference speed of left wheel motor, W is the width of wheelchair, K_l is the linear velocity gain, and K_a is the angular velocity gain.

5. EXPERIMENTAL RESULTS

Fig. 7 shows the developed DSP-based BLDC control module and electric power wheelchair.

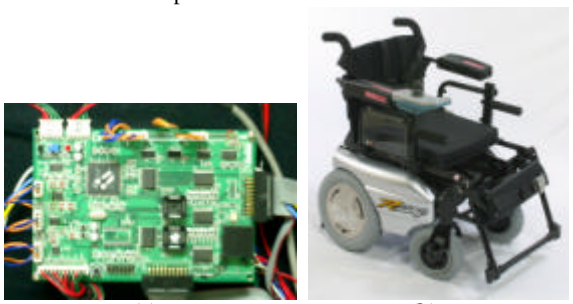

(a) (b)

Fig. 7 (a) DSP processor and three-phase inverter module, (b) Electric power wheelchair.

Fig. 8 shows the response of current control when the reference current is changed. The controller was implemented by PI algorithm and its cycle was 200 $m$sec .

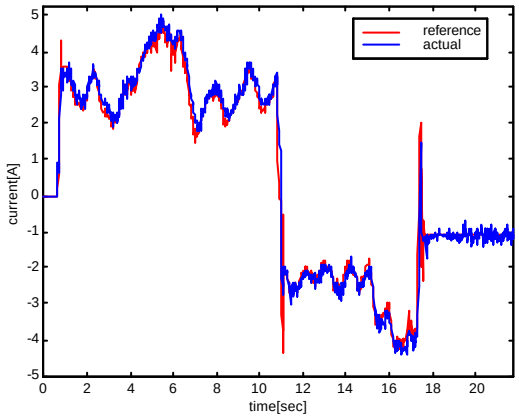

Fig. 8 Reference and actual current.

Fig. 9 shows the response of speed control when the reference speed is changed by the joystick.

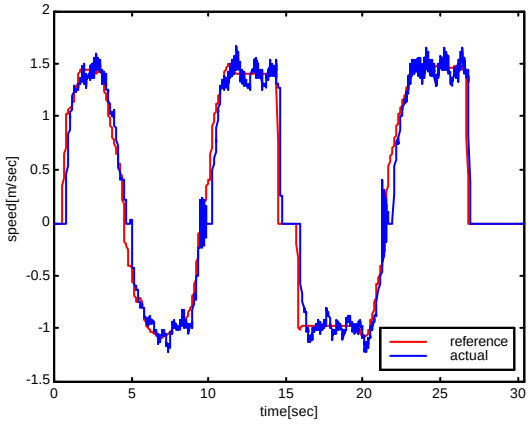

Fig. 9 Reference and actual speed.

We performed speed response experiments when an arbitrary reference speed was given by the joystick. Fig. 10 shows the joystick path, the reference and actual speed.

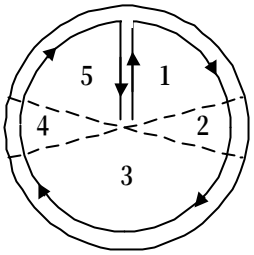

(a)

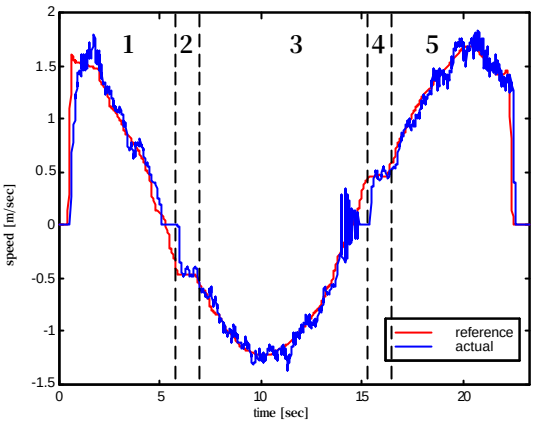

(b)

Fig. 10 (a) Joystick path, (b) Reference and actual speed.

6. CONCLUSION

In this paper, a method of torque and speed control for BLDC motor for the electric power wheelchair was presented. The reference speed profile was calculated by the joystick position and inverse kinematics. The current and speed controller was implemented using DSP and three-phase inverter module. By experiments, it can be verified that the proposed method is enough as a speed servo in wheelchair driving. Further work is in progress to generate a reference speed profile for comfortability.

REFERENCES

[1] S. J. Kang and S. K. Sul, "Direct Torque Control of Brushless DC Motor with Trapezoidal Back EMF," *IEEE Trans. on Power Electronics*, Vol. 10, No. 6, pp. 796-802, 1995.

[2] C. S. Berendsen, G. Champenois, and A. Bolopion, "Commutation Strategies for Brushless DC Motors: Influence on Instant Torque," *Trans. on Power Electronics*, Vol. 8, No. 2, pp. 231-236, 1993.

[3] R. Carson, M. Lajoie-Mazenc, and C. dos S. Fagundes, "Analysis of Torque Ripple Due to Phase Commutation in Brushless dc Machines," *IEEE Trans. on Industrial Application*, Vol. 28, No. 3, pp. 632-638, 1992.

[4] F. Blaabjerg, J. K. Pedersen, and U. Jaeger, and P. Thoegersen, "Single Current Sensor Technique in the DV Link of Three-Phase PWM-VS Inverters: A Review and a Novel Solution," *IEEE Trans. on Industrial Application*, Vol. 33, No. 5, pp. 1241-1253, 1997.